Review of Scientific Instruments

Development of a glue-free bimorph mirror for use in vacuum chambers

Cite as: Rev. Sci. Instrum. **90**, 021702 (2019); https://doi.org/10.1063/1.5066105
Submitted: 12 October 2018 . Accepted: 13 January 2019 . Published Online: 11 February 2019

Yoshio Ichii, Hiromi Okada, Hiroki Nakamori, Akihiko Ueda, Hiroyuki Yamaguchi, Satoshi Matsuyama, and Kazuto Yamauchi

Review of Scientific Instruments ARTICLE scitation.org/journal/rsi

Development of a glue-free bimorph mirror for use in vacuum chambers

Cite as: Rev. Sci. Instrum. 90, 021702 (2019); doi: 10.1063/1.5066105
Submitted: 12 October 2018 • Accepted: 13 January 2019 •
Published Online: 11 February 2019

Yoshio Ichii,[1,a)] Hiromi Okada,[1] Hiroki Nakamori,[1,2] Akihiko Ueda,[1] Hiroyuki Yamaguchi,[2] Satoshi Matsuyama,[2] and Kazuto Yamauchi[2]

AFFILIATIONS

[1]JTEC Corporation, 2-4-35 Saito-Yamabuki, Ibaraki, Osaka 567-0086, Japan
[2]Department of Precision Science and Technology, Graduate School of Engineering, Osaka University, 2-1, Yamadaoka, Suita, Osaka 565-0871, Japan

[a)]**Author to whom correspondence should be addressed:** yoshio.ichii@j-tec.co.jp

ABSTRACT

PZT (lead zirconate titanate)-glued bimorph deformable mirrors are widely used in hard X-ray regimes; however, they have not yet been used in soft X-ray regimes because they are less compatible for usage under high vacuum. In this study, we developed a glue-free bimorph deformable mirror, in which silver nano-particles were employed to bond PZT actuators to mirror substrates. Under an appropriate bonding condition, the bonding layer was confirmed to be uniform and the mirror's bending characteristics were demonstrated to be sufficiently stable; its gas emission rate was also shown to be acceptable. Piezo responses before and after additional heating at 200 °C showed the thermal stability of its bonding and bending properties.

I. INTRODUCTION

Third- and fourth-generation synchrotron radiation sources[1–3] provide extremely bright and coherent X-rays with a wide wavelength range, including soft and hard X-rays, and are used in various research fields of physics, chemistry, and biology. The field of precision optics is indispensable in enhancing the quality of X-ray analysis methods; it makes the X-ray beam as bright as possible and/or controls the flexibility of the beam's size. One of the mechanisms used for this purpose is a mirror with a mechanical bender; they have been used in beamline optical systems. However, the quality of their generated shape has been found to be insufficient due to the lack of controllability and instability of their bending devices. To overcome this issue, bimorph mirrors driven by piezo actuators are being developed since the 1990s.[4–8] These mirrors can equip a sufficient number of piezo actuators to finely modify the surface's shape to meet the necessary accuracy requirements. Accordingly, these newly developed deformable mirrors can generate nearly the exact shapes required to focus X-rays and/or to control the wavefront. As a practical example, Diamond Light Source (DLS) developed a method for using X-ray wavefront modification to change the beam size by using a deformable mirror that was nearly elliptically pre-shaped.[9–11] At SPring-8, a compensation optical system was developed that uses a bimorph mirror to realize an ultimate beam size of 7 nm. In this work, the diffraction-limited operation was realized in a compensational way, although the employed multi-layer coated[12,13] Kirkpatrick–Baez (KB) mirrors[14–19] did not fully satisfy the Rayleigh criterion.[20] Furthermore, a two-stage focusing optical system was used at SPring-8 to change the beam size, in which diffraction-limited performances were realized at all beam sizes.[21,22]

In these examples, epoxy glues were used in the fabrication of the bimorph mirrors to bond the piezo actuators (made of lead zirconate titanate, PZT) and the mirror substrate. This bonding method is suitable for use in hard X-ray optics, performed in ambient atmospheres. However, in the soft X-ray regime, the optics of which require high vacuum compatibility, glue cannot be used because of the gas emissions and denaturing of materials that occur at high temperatures. In this study, therefore, we have developed a glue-free bimorph mirror that can be used across a wide X-ray wavelength range, including soft X-rays.

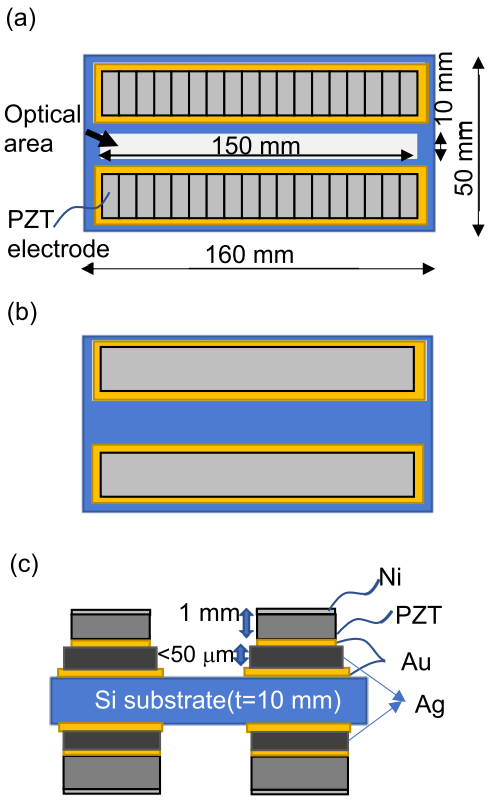

FIG. 1. Schematic image of the glue-free bimorph mirror developed in this study: (a) top surface (optical surface), (b) back side, and (c) cross-sectional view.

II. EXPERIMENTAL

The usual baking temperatures of vacuum chambers can be as high as 200 °C. For a bimorph mirror to maintain the characteristics at this temperature, the bonding material between the PZT (lead zirconate titanate) piezo actuators and the mirror substrate must not melt, become denatured, or emit gases at the baking temperature. In addition, bonding should be able to proceed at a lower temperature than Curie's temperature for PZT, which ranges from 280 to 330 °C. To meet these requirements, we employed silver (Ag) nanoparticles, which were first covered by alkoxide to give them a paste-like nature. They melt at ~250 °C (below Curie's temperature of PZT), after which they behave as a bulk-like metal, the melting point of which increases to 962 °C (i.e., significantly higher than the baking temperature).

Figure 1(a) shows the bimorph mirror developed in this study. The substrate is made of Si, with dimensions of 160 mm length, 50 mm width, and 10 mm thickness. X-rays are reflected at the center area of the upper flat surface, and the optical area is 150 mm in length and 10 mm in width. PZTs are bonded separately on both sides of the optical area, and the same PZTs are also bonded on the backside, as shown in Fig. 1(b); they are symmetrical in shape, so as to reduce unstableness due to thermal deformation. A schematic of the cross-sectional view of the stacking is shown in Fig. 1(c). The PZT and Ag layers are 1 mm and 50 μm thick, respectively. For bonding, both the surfaces of the PZT and the mirror substrate were coated with a 30-nm-thick gold (Au) film. This film enhances the bonding strength through the mutual diffusion of the Au and Ag layers. There are 18 electrodes on the PZTs on the upper surface, allowing for precise shape modification, and there is a large electrode on the back surface for global bending. Each electrode is wired to a DC multi-channel power supply, as shown in Fig. 2. Electrodes from Ch. 1 to 18 are on the upper surface, and the electrode of Ch. 20 is on the opposite surface. The electrode of Ch. 19 is on the backside of the PZTs that are to be grounded. The maximum applicable voltage of the PZTs is ±500 V.

Several bonding experiments were conducted under pressure conditions from 0.2 MPa to 10 MPa. The process temperature and time were 250 °C and 30 min, respectively. If void formation occurs in the Ag layer, then this could lead to the degradation of the bending characteristics. We, therefore, employed scanning acoustic tomography (SAT) to evaluate the uniformity of the Ag layer, and we evaluated gas emission properties via thermal desorption spectroscopy (TDS). In the TDS measurements, the temperature was increased to 200 °C during the first 15 min and was then kept at 200 °C for further 120 min. Each sample was kept at an ambient atmosphere for more than a week prior to the measurement. The piezo response relating to the uniformity of bonding layers was observed using a Fizeau interferometer (ZYGO GPI). In this observation, 500 V was applied to each electrode in sequence from Ch. 1 to 18; the electrodes of Ch. 19 and 20 were grounded. To understand the relationship between the applied voltage and the induced global curvature, we simultaneously applied the same voltage to the electrodes from Ch. 1 to 18 and observed the shapes recorded by using the Fizeau interferometer. The applied voltage was then increased sequentially from

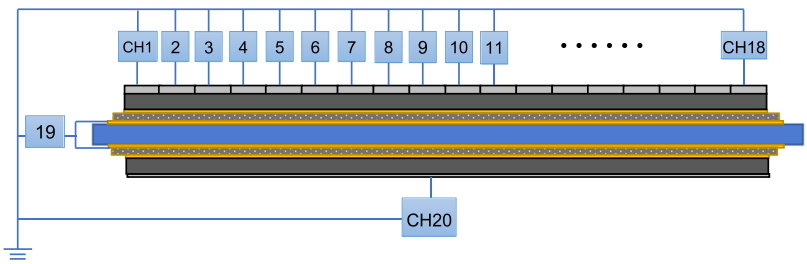

FIG. 2. Circuit image of the bimorph mirror. Ch 19 is grounded, and each electrode can be applied up to ±500 V.

20 V to 500 V, and the piezo response was also observed after additional heating to evaluate its influence.

III. RESULTS AND DISCUSSION

A. Bonding properties

Figures 3(a)–3(c) show the SAT images of samples prepared under pressure conditions of 0.2 MPa, 5 MPa, and 10 MPa, respectively. Figure 3(d) represents the positions of the PZTs relative to the mirror substrate. In Fig. 3(a), the uniformity of the Ag layer was relatively low due to a void formation; these voids were still observed at 5 MPa, as shown in Fig. 3(b). By contrast, no voids formed at 10 MPa, for which a uniform Ag layer was observed [Fig. 3(c)]. We therefore selected the pressure of 10 MPa for the following piezo response investigations.

B. Outgas characteristics

The obtained TDS spectra for carbon related gases are shown in Fig. 4. The profiles for mass-to-charge (m/z) ratios of 15, 18, 28, and 44 showed similar behaviors during the first 15 min, after which the signal intensities decreased significantly under the constant temperature of 200 °C. The organic molecules relating to alkoxides that were used as surface decoration materials for the Ag particles were not observed, implying that they had decomposed and/or desorbed during the bonding process at 250 °C. The final degree of vacuum

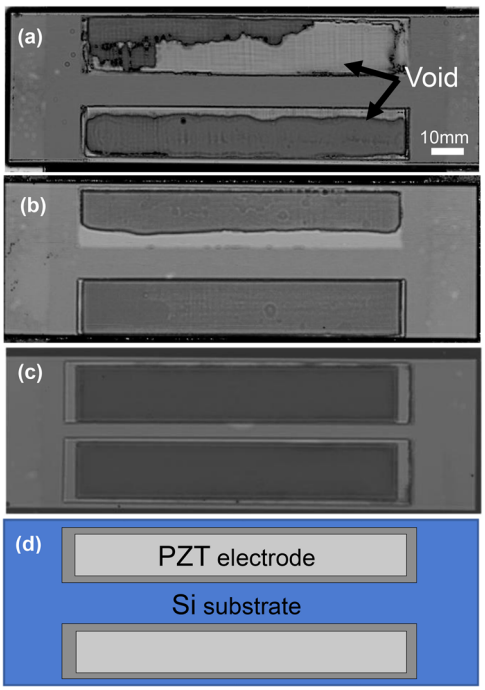

FIG. 3. SAT images of the Ag layer between the Si substrate and PZT, under pressure conditions of (a) 0.2 MPa, (b) 5 MPa, and (c) 10 MPa. (d) Position of the PZT electrode relative to the substrate. The arrow marks indicate the position of voids.

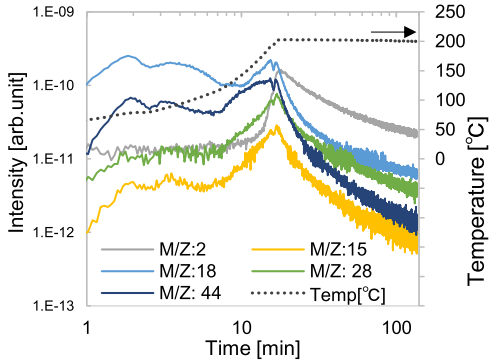

FIG. 4. TDS spectra of carbon-related gases throughout the experiment.

obtained for the TDS observations was 1.73×10^{-7} Pa; the gas emission rate estimated from this result was 5.2×10^{-8} Pa m^3/s. The sample size was 2×10^{-4} m^2. This result, while not excellent, would be acceptable for practical usage, and heating at 200 °C for 2 h could be used as a cleaning procedure for this bimorph mirror.

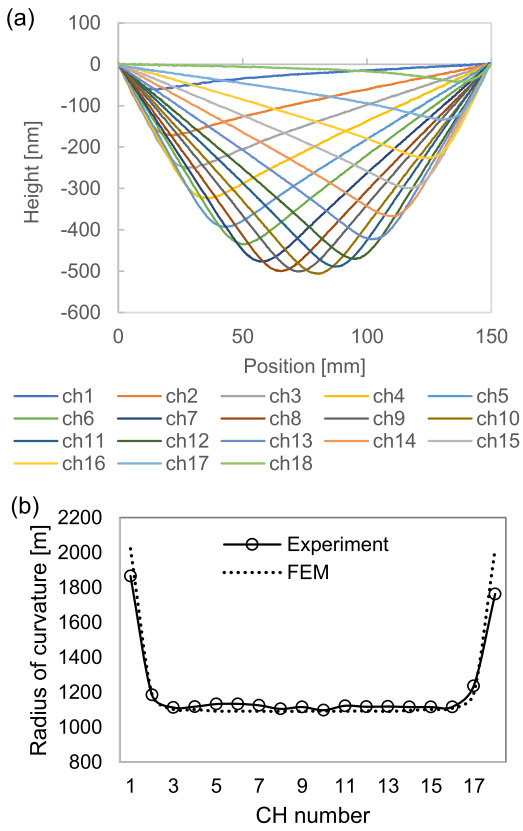

FIG. 5. (a) Piezo responses when 500 V is applied to each electrode in sequence and (b) the local ROCs estimated at each electrode (solid line with circles) and those calculated by FEM (dashed line).

C. Piezo responses

Figure 5(a) shows the piezo responses when 500 V was applied to each electrode in sequence. In elementary beam theory, the relationship between the moment, M, Young's modulus, Y_m, moment of inertia, I_m, and the induced radius of curvature (ROC), R, can be expressed as follows:

$$M = \frac{Y_m \cdot I_m}{R}. \quad (1)$$

The bending moment induced by a given electrode is proportional to the voltage applied to the electrode and is also proportional to the induced curvature at the position of the electrode. Accordingly, in the piezo responses shown in Fig. 5(a), the local ROC at the position of each electrode should be the same. The local ROCs estimated from Fig. 5(a) and those calculated via the finite element method (FEM) are shown in Fig. 5(b). There was good agreement for both ROCs, and nearly constant ROCs of ~1.12 km were observed at electrodes from Ch. 3 to 16. The deviation was smaller than 0.9%. However, the ROCs at electrodes of Ch. 1, 2, 17, and 18, which are placed at both ends of the substrate, increased significantly compared to those of the center area. This is due to the existence of stress fields at both ends, which are significantly different from those of the center area. Nearly 80% of the mirror can deform as expected and can therefore be used as an effective area. The effective area widened with decreasing thickness of the substrate, until the rigidity of the substrate became unacceptably low. Figure 6(a) shows the shapes formed when the same voltage was simultaneously applied to all of the electrodes from Ch. 1 to 18. The applied voltage was changed sequentially from 20 to 500 V in this experiment, and the electrodes of Ch. 19 and 20 were grounded. Figure 6(b) shows the relationship between the applied voltages and the induced curvatures. A linear relation can be clearly seen as expected from the theoretical calculations. The piezo response was measured again after being heated at 200 °C for 60 min to evaluate the influence of heating on the bending characteristics. A comparison between the local ROCs before and after heating is represented in Fig. 7. The mutual agreement is quite good, showing that heating at 200 °C did not affect either the bonding or the bending characteristics.

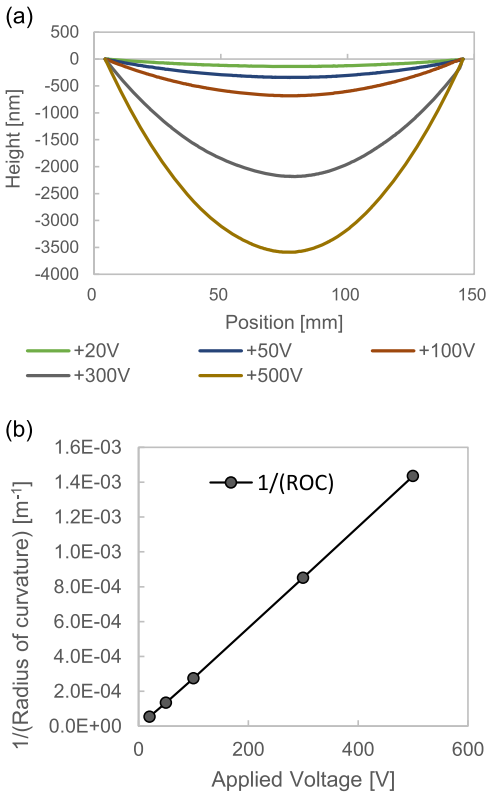

FIG. 6. (a) Mirror shape when the same voltage was simultaneously applied to all electrodes from Ch. 1 to 18. The applied voltage was from +20 V to +500 V. (b) Relationship between the applied voltages and induced curvatures of (a).

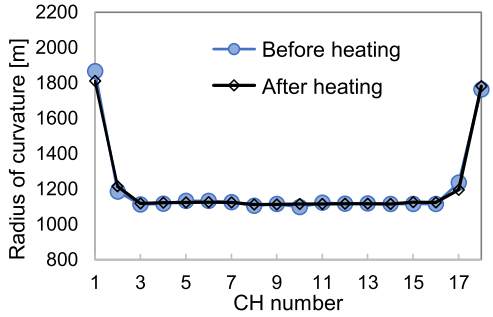

FIG. 7. The comparison between local curvatures before and after additional heating at 200 °C. The blue circles show the curvature before heating, whereas the black diamond patterns show curvature after heating.

IV. CONCLUSION

We developed a glue-free bimorph mirror that could be applied to X-ray beam steering in a high vacuum. Silver nanoparticles were employed as a substitute candidate material to bond PZT piezo actuators and the mirror substrate. Under appropriate bonding conditions, no voids were observed in the bonding layer, meaning that theoretically reasonable and stable bending characteristics were confirmed. Piezo responses before and after additional heating at 200 °C for 2 h demonstrated that our bimorph mirror is sufficiently stable under the heating required in soft X-ray regimes. We also evaluated its outgassing properties and confirmed that it is acceptable for usage in vacuums.

ACKNOWLEDGMENTS

This work was partially supported by a grant in aid from JSPS KAKENHI (Grant No. JP16H06358) and by the Hyogo Prefecture Center of Excellence program.

In addition, the authors would like to specially thank Mr. Matsumoto of Osaka University and Mr. Irisawa, Ms. Kiyomoto, Mr. Tsumura, and all members of JTEC Corporation.

REFERENCES

[1]Argonne National Laboratory, Conceptual Design Report Advanced Photon Source Upgrade Project, 2011.
[2]ESRF, ESRF Upgrade Program Phase II (2015-2019) White Paper, 2015.
[3]RIKEN/JASRI, SPring-8 Upgrade Plan Preliminary Report, 2012.
[4]R. Signorato, O. Hignette, and J. Goulon, J. Synchrotron Radiat. **5**, 797 (1998).
[5]J. Susini, D. Labergerie, and L. Zhang, Rev. Sci. Instrum. **66**, 2229 (1995).
[6]R. Signorato and T. Ishikawa, Nucl. Instrum. Methods Phys. Res., Sect. A **467-468**, 271 (2001).
[7]M. Idir, S. Fricker, M. H. Modi, and J. Potier, Nucl. Instrum. Methods Phys. Res., Sect. A **616**, 162 (2010).
[8]D. Cocco, G. Bortoletto, R. Sergo, G. Sostero, and I. Cudin, Nucl. Instrum. Methods Phys. Res., Sect. A **616**(2–3), 128 (2010).
[9]K. Sawhney, S. Alcock, J. Sutter, S. Berujon, H.-C. Wang, and R. Signorato, J. Phys. Conf. Ser. **425**, 052026 (2013).
[10]H.-C. Wang, K. Sawhney, S. Berujon, J. Sutter, S. G. Alcock, U. Wagner, and C. Rau, Opt. Lett. **39**(8), 2518 (2014).
[11]S. G. Alcock, I. Nistea, J. P. Sutter, K. Sawhney, J.-J. Fermé, C. Thellièr, and L. Peverini, J. Synchrotron Radiat. **22**(1), 10 (2015).
[12]C. Morawe, P. Pecci, J. C. Peffern, and E. Ziegler, Rev. Sci. Instrum. **70**, 3227 (1999).
[13]M. Störmer, H. Gabrisch, C. Horstmann, U. Heidorn, F. Hertlein, J. Wiesmann, F. Siewert, and A. Rack, Rev. Sci. Instrum. **87**, 051804 (2016).
[14]C. M. Kewish, L. Assoufid, A. T. Macrander, and J. Qian, Appl. Opt. **46**(11), 2010 (2007).
[15]W. Liu, G. E. Ice, L. Assoufid, C. Liu, B. Shi, R. Khachatryan, J. Qian, P. Zschack, J. Z. Tischler, and J.-Y. Choi, J. Synchrotron Radiat. **18**, 575 (2011).
[16]S. Yuan, V. V. Yashchuk, K. A. Goldberg, R. Celestre, W. R. McKinney, G. Y. Morrison, T. Warwick, and H. A. Padmore, Nucl. Instrum. Methods Phys. Res., Sect. A **649**(1), 160 (2011).
[17]T. Salditt, M. Osterhoff, M. Krenkel, R. N. Wilke, M. Priebe, M. Bartels, S. Kalbfleisch, and M. Sprung, J. Synchrotron Radiat. **22**, 867 (2015).
[18]J. C. Da Silva, A. Pacureanu, Y. Yang, S. Bohic, C. Morawe, R. Barrett, and P. Cloetens, Optica **4**(5), 492 (2017).
[19]G.-C. Yin, S.-H. Chang, B.-Y. Chen, H.-Y. Chen, B.-H. Lin, S.-C. Tseng, C.-Y. Lee, J.-X. Wu, S.-Y. Wu, and M.-T. Tang, Proc. SPIE **9592**, 959204 (2015).
[20]H. Mimura, S. Handa, T. Kimura, H. Yumoto, D. Yamakawa, H. Yokoyama, Y. Nishino, M. Yabashi, T. Ishikawa, and K. Yamauchi, Nat. Phys. **6**(2), 122 (2010).
[21]T. Kimura, S. Matsuyama, K. Yamauchi, and Y. Nishino, Opt. Express **21**(8), 9267 (2013).
[22]S. Matsuyama, H. Nakamori, T. Goto, T. Kimura, K. P. Khakurel, Y. Kohmura, Y. Sano, M. Yabashi, T. Ishikawa, Y. Nishino, and K. Yamauchi, Sci. Rep. **6**, 24801 (2016).